Picosecond excitation and selective intramolecular rates in supersonic molecular beams. IV. Alkylanthracenes

J. A. Syage, P. M. Felker,[a] D. H. Semmes, F. Al Adel, and A. H. Zewail[b]
Arthur Amos Noyes Laboratory of Chemical Physics,[c] California Institute of Technology, Pasadena, California 91125

(Received 5 November 1984; accepted 7 December 1984)

To assess the role of alkylation on IVR, the dynamics of jet cooled 9-methyl and 9-hexylanthracene excited to single vibronic levels (SVL) in S_1 are investigated and compared with the parent molecule, anthracene, whose picosecond IVR dynamics are now well characterized. Vibrations in S_1 and S_0 are analyzed. Decay rates and SVL fluorescence spectra are also presented. The decay rates as a function of excess vibrational energy increase rapidly at low energy but become relatively constant at high energy. The approximate energy threshold at which the decay rate "saturates" is dependent on the substitutent; anthracene ($\approx$1800 cm^{-1}), 9-methylanthracene ($\approx$1000 cm^{-1}), 9-hexylanthracene ($\approx$400 cm^{-1}), and A-$(CH_2)_3$-φ ($\leq$400 cm^{-1}). These identified thresholds are discussed and related to IVR processes. Finally, some comments on the importance of low frequency modes to IVR are given.

I. INTRODUCTION

This paper represents a continuation of work dealing with the picosecond time-resolved measurements[1-4] of intramolecular processes in jet-cooled large molecules. In the first paper (I) of the series,[2] single vibronic level (SVL) fluorescence spectra and excited state lifetimes were reported for anthracene and deuterated anthracenes. In the second paper (II),[3] a detailed study of quantum beats in anthracene was discussed. In papers I and II, the central focus was on the problem of intramolecular vibrational redistribution (IVR). In the third paper of the series (III),[4] a novel photochemical system was reported entailing a charge transfer (or exciplex) reaction that occurs in the molecule anthracene-$(CH_2)_3$-*N*,*N*-dimethylaniline [*A*-$(CH_2)_3$-φ]. In this system, the chain dynamics involved in the charge transfer reaction were investigated. In the present paper (IV), we present our results on the spectroscopy and chain dynamics of alkyl substituted anthracenes where there is no charge transfer. Since anthracene spectroscopy[6] and IVR dynamics[2,3] are now well characterized, it is of interest to examine the role of IVR in alkylanthracenes. Although these studies involve unreactive systems, the insights gained here shed light on the role of IVR in reactive systems. They furthermore relate to the time-integrated work by Smalley's group on alkylbenzenes,[5] as discussed later.

We begin by presenting the 0^0 level excitation and dispersed fluorescence spectra of 9-methylanthracene and 9-hexylanthracene in order to understand the important vibrations of these molecules and to make comparisons with our previous findings on anthracene and *A*-$(CH_2)_3$-φ. The SVL fluorescence spectra and the direct time-resolved measurements of the vibronic lifetimes are then interpreted in terms of the coupling of the initially excited level with an effective density of states. The molecule 9-methylanthracene is also of interest from the standpoint of the methyl torsion. In toluene (methylbenzene), the barrier to rotation is a mere 5 cm^{-1}.[7] A jet-cooled study of toluene has revealed the presence of low frequency torsional levels[8] which exhibit energy spacings and selection rules characteristic of rotations. We examine the low frequency modes of 9-methylanthracene in terms of possible models for the methyl torsional barrier. Finally, we discuss, in a systematic manner, the nature of IVR in these systems.

II. EXPERIMENTAL

The 9-methylanthracene (Alfa, 99%) was used as is. The 9-hexylanthracene was obtained from the University of Bordeaux, courtesy of the organic chemistry group (courtesy of Dr. Desvergne and Dr. Bouas-Laurent). The purity following recrystallization in CCl_4 was determined by gas chromatography to be 95% (the major impurity was anthracene: 4.5%). Two sets of supersonic beam apparatus were used to record the spectra in this paper and are described in detail elsewhere.[3,4,9] A pulsed jet system[4,9] was used to record the excitation spectra. A continuous jet system[3] was employed to record dispersed fluorescence and time-resolved spectra. We give a brief description below.

A. Pulsed jet apparatus

The pulsed jet relies on a low inductance solenoid modified to deliver pulse widths of typically 250 μs when driven by a pulsed amplifier (10 kW peak power). A digital temperature controller is used to maintain the nozzle temperature to better than 1 °C. A YAG pumped dye laser (5 ns pulses) was operated at 15 Hz. UV pulses were generated with a KDP crystal whose angle was

[a] IBM Predoctoral Fellow.
[b] Camille and Henry Dreyfus Foundation Teacher-Scholar.
[c] Contribution No. 7093.

 0021-9606/85/072896-13$02.10 © 1985 American Institute of Physics

Downloaded 21 Sep 2008 to 131.215.225.9. Redistribution subject to AIP license or copyright; see http://jcp.aip.org/jcp/copyright.jsp

optimized via a computer controlled feedback system, thus allowing continuous UV scans.

Excitation spectra were recorded using jet expansions involving 50 psi backing pressures of He or Ne through a 300 μm aperture. The nozzle-to-laser distance was maintained at 1.5–2.0 cm where cooling was determined to be optimum as indicated by constant rotational bandwidths and hot band intensities at longer distances. Spectra were also recorded by varying the backing pressures of these and other carrier gases (i.e., N_2 and Ar) as well as the nozzle-to-laser distance in order to examine the effect of different cooling conditions on the observed spectra. The compounds 9-methylanthracene and 9-hexylanthracene were heated to temperatures of about 140 and 160 °C, respectively. Our compact beam is pumped by a 4 in. diffusion pump which maintained an ambient pressure in the expansion chamber of $\leq 5 \times 10^{-4}$ Torr.

The excitation spectra were recorded by collecting the fluorescence via $f/1$ optics through Schott WG395 and Corning 0-51 cutoff filters and a Corning 7-51 bandpass filter to eliminate scattered laser light. The UV fluorescence was detected by an EMI6256B PMT. The fluorescence signal was normalized with respect to laser intensity using a 1P28 PMT, which detected a small portion of the UV laser output. The PMT outputs were fed into a dual channel boxcar integrator. The normalized output was then digitized by a voltage to frequency converter and stored on floppy disks.

B. Continuous jet apparatus

The continuous jet apparatus is equipped with a 12 in. ring jet diffusion pump capable of maintaining 10^{-4} Torr ambient pressure during normal operation. The jet is excited with a picosecond dye laser, synchronously pumped by a mode-locked argon ion laser. The dye pulses were cavity dumped (variable from 0.8 to 4 MHz) and frequency doubled with $LiIO_3$ to give UV pulses with temporal and frequency pulse widths (FWHM) of $\approx$15 ps and $\approx$0.3 Å, respectively. The pulse energy in the visible is $\sim$10 nJ.

The 9-methylanthracene and 9-hexylanthracene were heated to about 140 and 200 °C, respectively, and expanded through a 150 μm pinhole. All expansions in the continuous jet were backed by 35 psi of either He or Ne unless otherwise noted. Excitation of the jet cooled molecules occurred 4–5 mm from the nozzle where it was determined that collision-free conditions had been attained. The fluorescence was collected using $f/1$ optics and imaged onto a microprocessor-controlled 0.5 m monochromator and detected by a photon counting PMT. Data were collected on a multichannel analyzer and transferred to a PDP 11/23.

C. Wavelength calibration and treatment of data

The dye laser and monochromator wavelength scales were calibrated against known Ne lines observed in a Fe–Ne discharge lamp (see Refs. 3 and 4 for further details). The vibrational modes observed in the excitation spectra are reported to an accuracy of 1 cm^{-1} or 0.1%, whichever is larger. Assignments from the dispersed fluorescence spectra are reported to an accuracy of 5–10 cm^{-1}. No vacuum corrections have been made. The relative intensities in the resolved fluorescence spectra have not been corrected for the spectral response of the PMT.

Time-resolved fluorescence was obtained using single photon counting. The quality of the exponential fits was uniformly excellent as judged by the reduced χ^2 values and the weighted residuals which display the point-by-point deviations of the experimental curve from the fitted curve. The data presented here represent an average over many determinations and are reported with their standard deviation.

III. RESULTS AND ANALYSIS

A. Analysis of S_0 and S_1 vibrations

1. Preliminaries and general features

We adopt Pariser's notation[10] for the molecular axis system of anthracene such that the out-of-plane axis is "z," the short in-plane axis "y," and the long in-plane axis "x." In this system the first excited electronic state of anthracene reported here is $^1B_{2u}$ (in D_{2h}). The transition dipole moment for $S_1 \leftarrow S_0$ lies along the short in-plane y axis and corresponds to the $^1B_{2u}^+ (\pi\pi^*) \leftarrow {}^1A_g^-$ transition.[6,11] The vibrationless electronic transition (i.e., the 0_0^0) was detected at 3712.0 and 3730.3 Å for 9-methylanthracene (9-MA) and 9-hexylanthracene (9-HA), respectively. This is to be compared with our measured values for anthracene[6] and 9-(3-(4-(*N*,*N*-dimethylaniline))propyl)anthracene [henceforth *A*-$(CH_2)_3$-φ][4] of 3610.7 and 3747.7 Å, respectively.

For strict D_{2h} symmetry and in the absence of vibronic coupling, only a_g modes are allowed for the B_{2u}–A_g electronic transition. A Herzberg–Teller coupling with a relatively low lying $^1B_{3u}$ state with strong oscillator strength has been observed to induce b_{1g} vibrational activity.[6,12] There are 12 a_g modes in anthracene. Three of these correspond to C–H stretching modes which are inactive for π, π^* excitation. We designate anthracene-like vibrations by the notation used by Stockburger and others[13,14] in which the a_g vibrations are labeled numerically from high to low frequency. The vibronically induced b_{1g} vibrations are also represented as integers but with a bar above them. We refer to vibronic transitions as A_n^m where A is the mode number and n and m are the number of quanta of mode A in the ground and excited electronic state, respectively. Combination bands are consequently expressed as $A_n^m B_{n'}^{m'} \cdots$ and excited state single vibronic levels as $A^m B^{m'} \cdots$.

The excitation and dispersed fluorescence spectra of 9-MA and 9-HA are illustrated and compared with anthracene in Figs. 1 and 2. The band frequencies, intensities, and assignments in excitation and fluorescence are compiled in Tables I and II, respectively. As discussed in an earlier paper[4] the spectra of the substituted anthracenes (effectively C_{2v}) are similar to anthracene (D_{2h}) indicating that the substituents have a relatively minor influence on the electronic and vibrational states of anthracene. The

Downloaded 21 Sep 2008 to 131.215.225.9. Redistribution subject to AIP license or copyright; see http://jcp.aip.org/jcp/copyright.jsp

insensitivity of the anthryl-type vibrational frequencies to the 9-substituents is evident in the comparison of frequencies for anthracene, 9-methylanthracene and 9-hexylanthracene and A-$(CH_2)_3$-φ[4] in Table III. The presence of low frequency bands in the excitation spectra of the substituted anthracenes, however, indicates that chain motions *do* have some interaction with the electronic structure. As shown in Fig. 3, some differences among the S_1 C–C stretch modes at about 1400–1500 cm^{-1} exist.

2. Vibrational cooling and complexes

The degree of vibrational cooling in supersonic jet expansions generally varies for different vibrations and depends on the carrier gas and backing pressure. Weak features due to hot molecule absorptions (hot bands) and van der Waals complexes between seed and carrier molecules can occur. Since the substituted anthracenes undergo low frequency vibrations of importance to this study, it is imperative to distinguish these absorptions from those associated with hot bands and complexes. Consequently, we have recorded a series of spectra under various expansion conditions to address this issue.

a. van der Waals complexes. The formation of van der Waals complexes were particularly evident in the excitation spectra of 9-hexylanthracene which gave rise to extensive bonding interactions with Ar and N_2 (and to a lesser extent with Ne). Excitation spectra of the 0_0^0 region of 9-HA as a function of Ar backing pressure are given in Fig. 4. Complexes involving increasing numbers n of Ar atoms are clearly resolved and red shifted by 48, 89, and 132 cm^{-1}. The van der Waals bands are sharp but broaden as n increases (particularly for $n > 3$). The

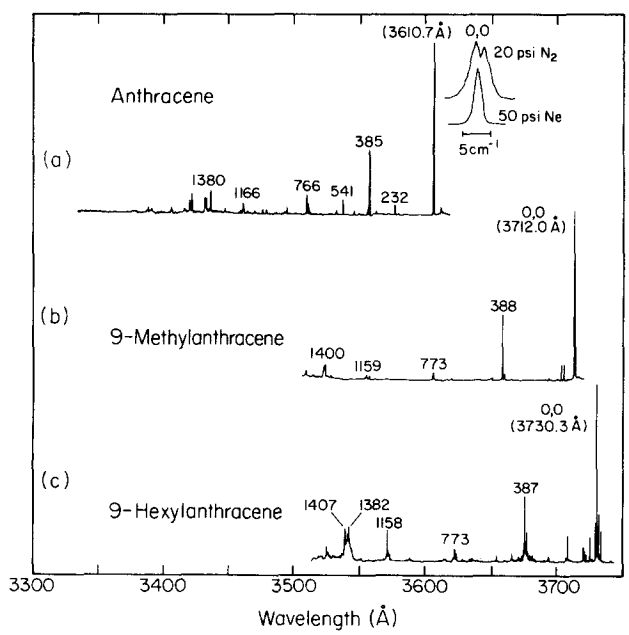

FIG. 1. Excitation spectra for the $B_{2u} \leftarrow A_g$ electronic transition of (a) anthracene; expansion conditions were 50 psi N_2 and 130 °C, (b) 9-methylanthracene; 50 psi He and 140 °C, (c) 9-hexylanthracene; 50 psi Ne and 160 °C. All other conditions are given in the experimental section. The rotational band shape of the 0_0^0 transition of anthracene is illustrated under two different cooling conditions. The wavelength scale is approximate.

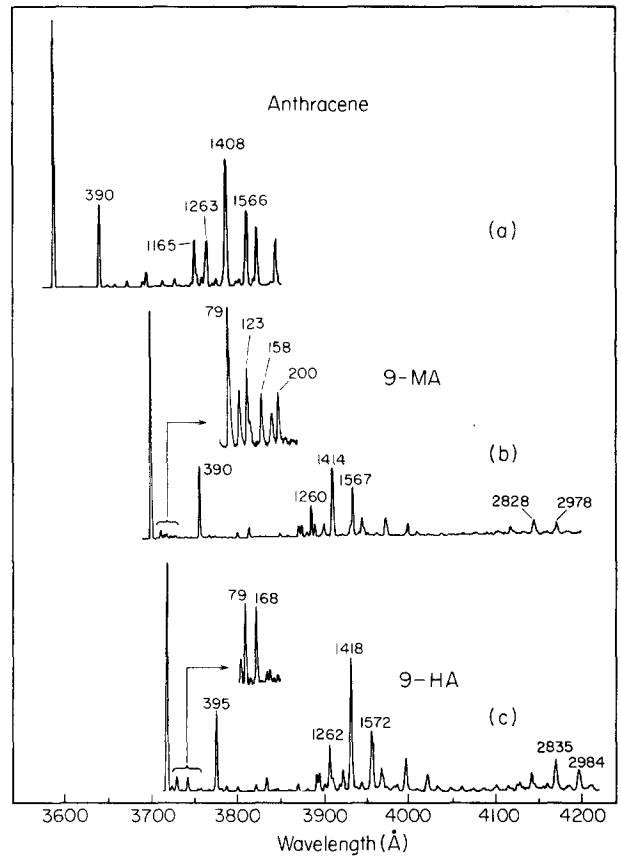

FIG. 2. 0^0 level dispersed fluorescence spectra, (a) anthracene: 45 psi N_2, 105 °C; (b) 9-Methylanthracene: 35 psi He, 140 °C; (b) 9-hexylanthracene: 35 psi He, 200 °C. Monochromator resolution was 1.0 Å for all spectra.

van der Waals complex band involving Ne was sharp and red shifted by 60 cm^{-1}, however, those of the N_2 complexes were completely broad. The formation of van der Waals complexes with 9-MA was less prevalent, but the spectral features exhibited were similar to those observed for 9-HA. These spectroscopic features have been well studied for other systems such as tetracene and fluorene by Even and Jortner.[15] For the anthracene origin, Schlag's group reported detailed studies of complexes with Ar.[16] The implications of our results to IVR are discussed in Sec. IV A 2 with focus on chain modes in alkylanthracenes.

b. Torsion bands and hot bands. The vibrational cooling in 9-HA, from the standpoint of diminished hot band intensities, is judged to be quite good for all carrier gases at high pressures. We illustrate this in Fig. 5 by showing excitation spectra of the 0_0^0 region as a function of He backing pressure (a carrier gas which does not form any apparent van der Waals complexes). At low pressure, rotational cooling is poor and substantial broadening results. Rotational cooling improves with Ne and Ar at equivalent pressures, however, these gases give rise to van der Waals complexes (Fig. 4). It is important to note that the relative intensities of the several bands about the 0_0^0 remain unchanged as a function of backing pressure indicating that they are probably not due to hot bands. This does not rule out the possibility that some of these bands are due to modes that do not cool efficiently in the

Downloaded 21 Sep 2008 to 131.215.225.9. Redistribution subject to AIP license or copyright; see http://jcp.aip.org/jcp/copyright.jsp

TABLE I. Prominent features in the excitation spectra of 9-methylanthracene and 9-hexylanthracene.

9-Methylanthracene			9-Hexylanthracene		
Frequency[a] (cm^{-1})	Relative intensity	Assignment[b]	Frequency[a] (cm^{-1})	Relative intensity	Assignment[b]
			−24	17	
			−15	3	
			−10	29	
			−5	16	
0	100	0_0^0	0	100	0_0^0
56	13		7	22	
69	14		36	12	
125	2		38	5	
157	2		64	5	
373	5		72	6	
388	45	12_0^1			
443	3	(56) } +388	157	12	
456	2	(69) }			
672	2	10_0^1?			
773	6	12_0^2	371	4	
			377	13	12_0^1 −15
			387	34	12_0^1 −10
			395	5	12_0^1 0, +7
1159	4	8_0^1	458	3	(72) } +387
			543	3	(157) }
1360	2		765	3	
1400	9	6_0^1	773	5	12_0^2 −10, 0, +7
1405	8	5_0^1	780	2	
			1148	2	
			1154	3	8_0^1 −10, −5, 0, +7
1512	4	4_0^1	1158	14	
			1166	3	
			1373	3	
			1380	8	6_0^1 −10, −5, 0, +7
			1382	8	
			1390	5	
			1402	8	
			1407	15	5_0^1
			1512	4	4_0^1

[a] Frequencies are reported relative to the 0_0^0 to an accuracy of 2 cm^{-1}.
[b] Modes of uncertain assignment that appear in combinations are enclosed in parentheses ( ) with their frequency.

expansion process or due to different conformers of the chain.

Vibrational cooling in 9-MA is not as good as in 9-HA. We have found from experience that longer chain molecules and molecules with many low frequency modes cool better. This may be due to the ability of these molecules to dispose of vibrational energy in smaller more efficient increments. We display 0_0^0 excitation spectra in Fig. 6 as a function of He backing pressure to illustrate the emergence of several resolvable hot band features at low pressure, both to the red and the blue of the true 0_0^0. Part of the structure is probably due to partially resolved *B*-type rotational structure of the kind observed in jet-cooled anthracene[6] on account of the short axis polarization of the $^1B_{2u} \leftarrow {}^1A_g$ transition [cf. Fig. 1(a)]. This splitting is clearly evident in less congested bands of 9-MA (cf. Figs. 7 and 8). Finally, we mention that the lifetimes of the bands that overlap with the 0_0^0 vary widely (Fig. 6), possibly because the excitations involve a number of excited state modes.

Prominent (hot) bands to the blue of the 0_0^0 in 9-MA were observed at 31 and 83 cm^{-1} and exhibited a strong dependence on cooling conditions (Fig. 8). A very similar set of bands were observed in a study of jet-cooled toluene[8] (i.e., methylbenzene) which were attributed to excitations between methyl torsional levels in S_0 and S_1. In toluene, the torsional band frequencies satisfied the selection rules and rotational spacings expected for a free methyl rotor. This observation in toluene was analyzed in terms of a low barrier to methyl rotation of ≈ 5 cm^{-1} which was reported in other studies.[7] The torsional band frequencies observed for 9-MA in the present work differ from those in toluene presumably due to a larger barrier (likely) or a different rotational constant (unlikely) for methyl rotation.

3. Low frequency modes

a. 9-Methylanthracene. Two relatively prominent modes which appear as a doublet are evident at 56 and 69 cm^{-1} (Figs. 7 and 8). The SVL dispersed fluorescence spectra in Fig. 9 indicate that these modes correspond to

Downloaded 21 Sep 2008 to 131.215.225.9. Redistribution subject to AIP license or copyright; see http://jcp.aip.org/jcp/copyright.jsp

TABLE II. Prominent features in the dispersed fluorescence spectra of 9-methylanthracene and 9-hexylanthracene.

9-Methylanthracene			9-Hexylanthracene		
Frequency[a] (cm^{-1})	Relative intensity	Assignment	Frequency[a] (cm^{-1})	Relative intensity	Assignment
0	100	0_0^0	0	100	0_0^0
79	4		43	2	
104	2		79	7	
123	2		168	6	
390	32	12_1^0			
694	3	10_1^0?	395	35	12_1^0
786	5	12_2^0			
1024	2	9_1^0?	477	3	
1164	5	8_1^0	711	3	
1184	6	$\overline{7}_1^0$?	789	6	12_2^0
1224	3		1028	4	9_1^0?
1260	14	7_1^0	1167	8	8_1^0
1283	6		1187	8	$\overline{7}_1^0$?
1356	6		1229	4	
1414	31	6_1^0	1262	21	7_1^0
1567	22	4_1^0	1337	3	
1634	9	$\overline{3}_1^0$	1360	10	
1806	8	$6_1^0 12_1^0$	1418	49	6_1^0
1963	6	$4_1^0 12_1^0$	1498	5	5_1^0
2025	2	$\overline{3}_1^0 12_1^0$	1572	27	4_1^0
2198	2	$6_1^0 12_1^0$	1639	11	$\overline{3}_1^0$
			1812	15	$6_1^0 12_1^0$
2673	4	$6_1^0 7_1^0$	1964	8	$4_1^0 12_1^0$
2828	7	6_2^0	2032	3	$\overline{3}_1^0 12_1^0$
		$6_1^0 5_1^0$	2203	3	$6_1^0 12_2^0$
2978	6	$6_1^0 4_1^0$	2442	4	
			2579	4	
			2597	5	
			2676	9	$6_1^0 7_1^0$
			2778	4	
			2835	12	6_2^0
			2921	3	$6_1^0 5_1^0$
			2984	9	$6_1^0 4_1^0$

[a] Frequencies are reported relative to the 0_0^0 to an accuracy of 5–10 cm^{-1}.

S_0 modes at 79 and 104 cm^{-1}, respectively. The absence of such low frequency bands in anthracene can be taken as evidence for the involvement of the methyl group in the vibrational motion. The assignment of the modes cannot be determined with certainty, however, we can be guided by certain considerations. For instance, it is not likely that the vibrations correspond to a_g motions in D_{2h} symmetry since this could only be satisfied by an anthracene–methyl stretch motion which would have higher frequencies than those observed. Vibronically induced b_{1g} vibrations which allow for methyl (in-plane) bend motion could account for lower frequencies. It is also conceivable that vibrations that strongly involve the methyl group may be best represented in C_{2v} symmetry (or some local methyl symmetry), thus relaxing somewhat the D_{2h} selection rules. For instance, both a_g and b_{2u} vibrations in D_{2h} transform as totally symmetric a_1 modes in the approximate C_{2v} symmetry arising from substitution at position 9. A local methyl symmetry such as C_3 might allow for optically active low frequency out-of-plane motion.[17] One might also speculate that the observed modes may have a composite (in-plane) methyl–anthryl rocking motions. It is interesting to note, however, that the frequencies differ markedly in S_0 and S_1 indicating that a significant change in the potential for these modes occurs upon electronic excitation.

The possibility that hindered internal methyl rotation might account for the observed frequencies is worth considering, even though this motion is essentially a free rotor in methylbenzene (i.e., barrier is ≈ 5 cm^{-1}).[7] We may estimate the barrier to internal rotation that would be necessary to account for the observed frequencies using a simple model for hindered internal rotors.[18] For symmetric harmonic motion, the potential for internal rotation may be described by

$$V(\alpha) = \tfrac{1}{2} V_N (1 - \cos N\alpha), \tag{1}$$

where V_N is the barrier height between minima and N is the number of minima.[18] The frequency of the hindered rotor is then given by

$$\nu_T\,(\mathrm{cm}^{-1}) = \frac{N}{2\pi}\left[\frac{V_N}{2I_R}\right]^{1/2}. \tag{2}$$

Downloaded 21 Sep 2008 to 131.215.225.9. Redistribution subject to AIP license or copyright; see http://jcp.aip.org/jcp/copyright.jsp

TABLE III. Comparison of major vibrational frequencies for anthracene derivatives.

Mode		Anthracene	9-Methyl Anthracene	9-Hexyl Anthracene	A-$(CH_2)_3$-φ
ν_{12}	gnd	390	390	395	386
	exc	385	388	387	392
ν_{11}	gnd	624			
	exc	583			
ν_{10}	gnd	753	694 ?		
	exc	755	672 ?		
ν_9	gnd	1012	1024 ?	1028 ?	1008 ?
	exc	1019			
ν_8	gnd	1165	1164	1167	1167
	exc	1168	1159	1158	1159
ν_7	gnd	1263	1260	1262	1254
	exc	1168 ?			
ν_6	gnd	1408	1414	1418	1407
	exc	1380	1400	1382	1380
ν_5	gnd	1486		1498	
	exc	1420	1405	1407	1393 ?
ν_4	gnd	1566	1567	1572	1565
	exc	1501	1512	1512	1499

I_R is the reduced moment of inertia for a given torsion and can be determined by the relation

$$I_R = \frac{I_1 I_2}{I_1 + I_2}, \tag{3}$$

where I_1 and I_2 are the moments of inertia about the torsional axis of the two parts of the molecule involved in the motion. For the overall sixfold (i.e., $N = 6$) methyl–anthryl torsional potential, one obtains the result V_N (cm^{-1}) = $(\nu_T)^2/33$ (where the units of ν_T and the denominator are cm^{-1}). The potential barrier to methyl rotation must therefore be in the vicinity of 100 cm^{-1} in order to attribute this vibration to one of the observed bands at 56 or 69 cm^{-1}.

It is not clear what effect the interaction of the additional hydrogens on the outer rings of anthracene will have on the barrier to methyl rotation compared to that in methylbenzene. One might expect the barrier to increase, but not substantially. Evidence from other systems[19] indicates that the barrier to methyl rotation is substantially smaller when the adjacent twofold substituent is symmetric rather than asymmetric. A relatively small barrier of 100 cm^{-1} is consistent with these qualitative considerations, however, it is still substantially larger than the barrier of 5 cm^{-1} reported for toluene.[7] The frequencies of the torsional hot bands observed for 9-MA (Sec. III A 2), however, are also consistent with a barrier to methyl rotation that is greater than in toluene. Unfortunately, it is not possible with the information at hand to obtain a good estimate of this value. It would be interesting to study methyl rotation in 1-methylanthracene or methylnaphthalene in order to address the effect of the symmetry of the internal rotors on the torsional barrier.

b. 9-Hexylanthracene. In Fig. 5, we examine the very low frequency modes of 9-HA under various cooling conditions. On the basis of the insensitivity of the relative intensities to different vibrational temperatures it is concluded that these bands are probably not hot bands (unless they represent modes that cool inefficiently during the expansion), but are either fundamentals or different conformers of the molecule. Conformers may equilibrate at a much slower rate than vibrations and rotations and hence a distribution can become "frozen in" during a jet expansion if the cooling rate is sufficiently fast. Consequently, the ratio of different conformers may not be sensitive to the final cooling characteristics of the expansion. An example of this effect is evident in the jet-cooled spectra of alkylbenzenes reported by Smalley *et al.*[5] We have likewise found evidence for the presence of more than one conformer in the jet-cooled excitation spectra of A-$(CH_2)_3$-φ[4] and *t*-stilbene.[20]

Although the presence of different conformers of 9-HA in our jet spectra is reasonable, the large number of low frequency bands would seem to require some assignments as fundamental vibrations. Unlike 9-MA the asymmetry of an alkyl rotor imparts a significant potential to

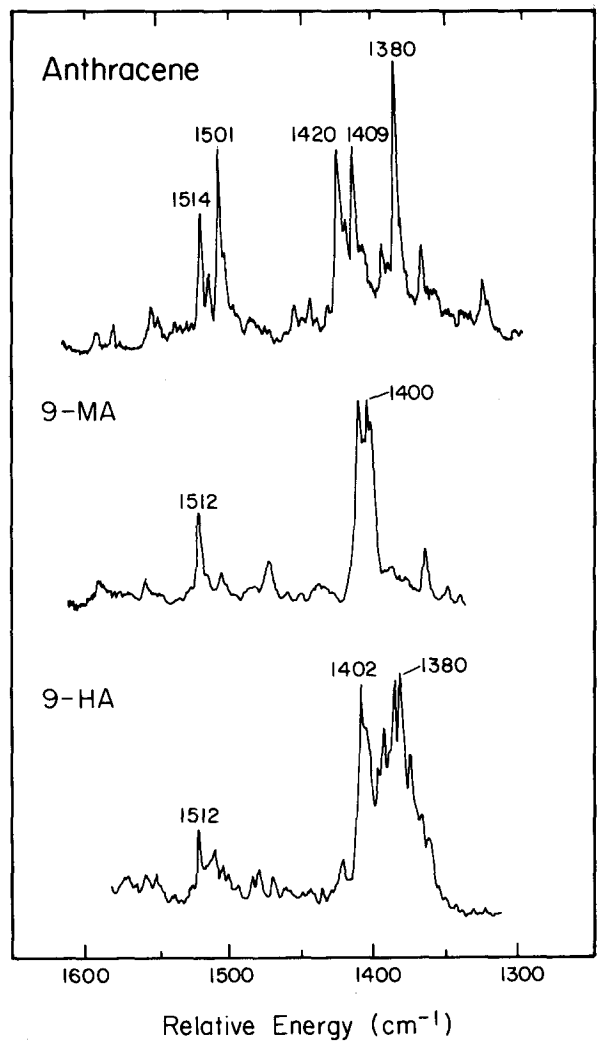

FIG. 3. Comparison of the C–C stretch vibrations in excitation for the series of anthracene derivatives discussed in this work. All spectra were recorded under 50 psi He except for anthracene (50 psi Ne).

Downloaded 21 Sep 2008 to 131.215.225.9. Redistribution subject to AIP license or copyright; see http://jcp.aip.org/jcp/copyright.jsp

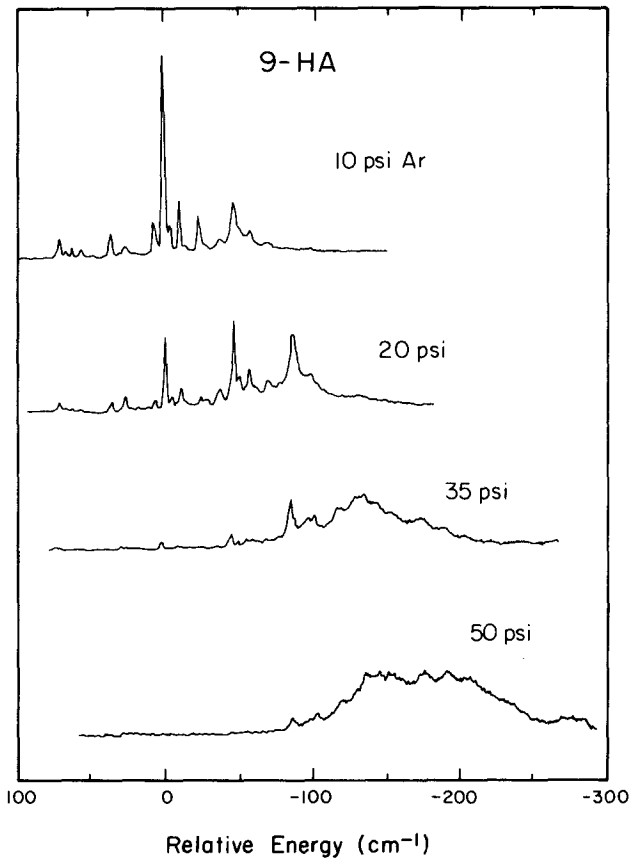

FIG. 4. Excitation spectra of the 0_0^0 region of 9-hexylanthracene as a function of Ar backing pressure. Spectra illustrate van der Waals complexes involving successively larger number of Ar atoms.

internal rotation.[19] For instance, in ethylbenzene, this barrier has been determined to be 400–600 cm^{-1}.[21] For longer alkyl groups interacting with larger aromatics (e.g.,

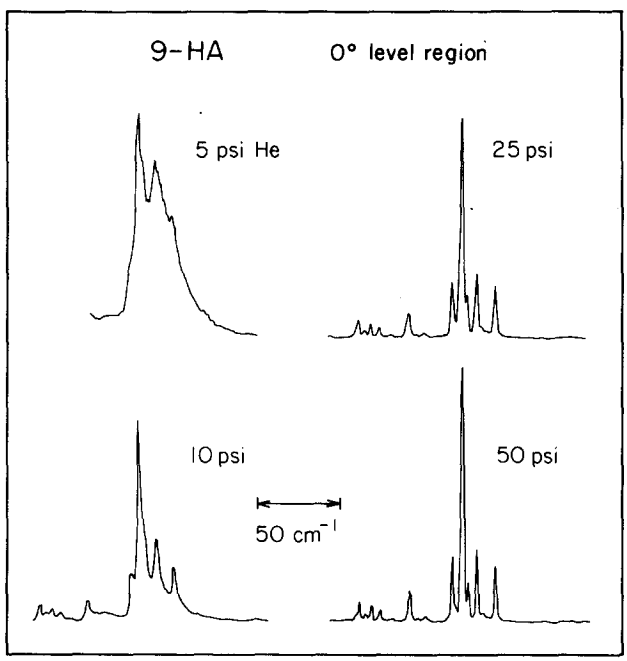

FIG. 5. Excitation spectra of the 0_0^0 region of 9-hexylanthracene as a function of He backing pressure. Relative intensities of the low frequency bands are unaffected by pressure indicating that they are probably not hot bands. Note absence of van der Waals complexes with He.

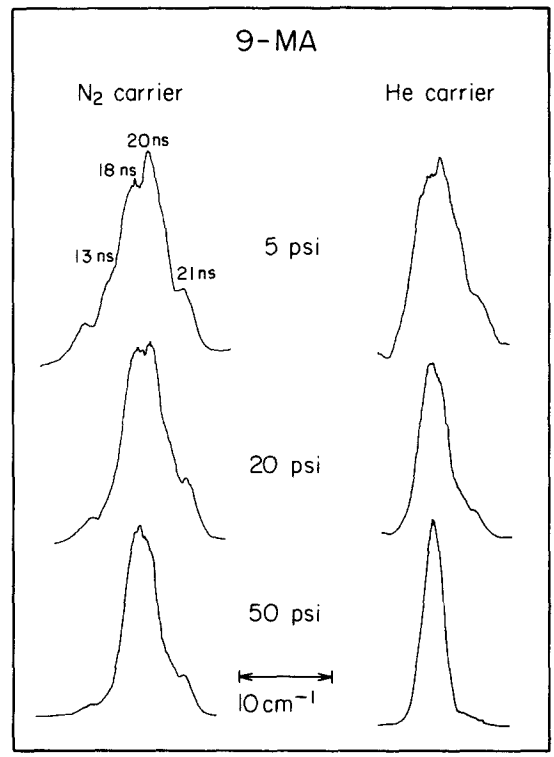

FIG. 6. Excitation spectra of the 0_0^0 region of 9-methylanthracene as a function of N_2 and He backing pressure. Note the presence of several bands at low pressure, presumably due to hot band transitions involving methyl torsional levels. Measured decay times for different regions of the band shape are indicated for 5 psi N_2.

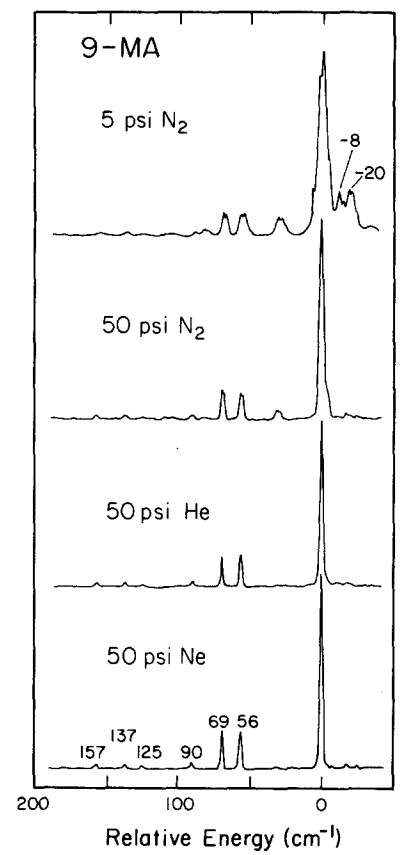

FIG. 7. Excitation spectra of the low energy region of 9-methylanthracene as a function of carrier gas and backing pressure. The emergence of hot band transitions involving methyl torsional levels is clearly evident under reduced cooling conditions.

Downloaded 21 Sep 2008 to 131.215.225.9. Redistribution subject to AIP license or copyright; see http://jcp.aip.org/jcp/copyright.jsp

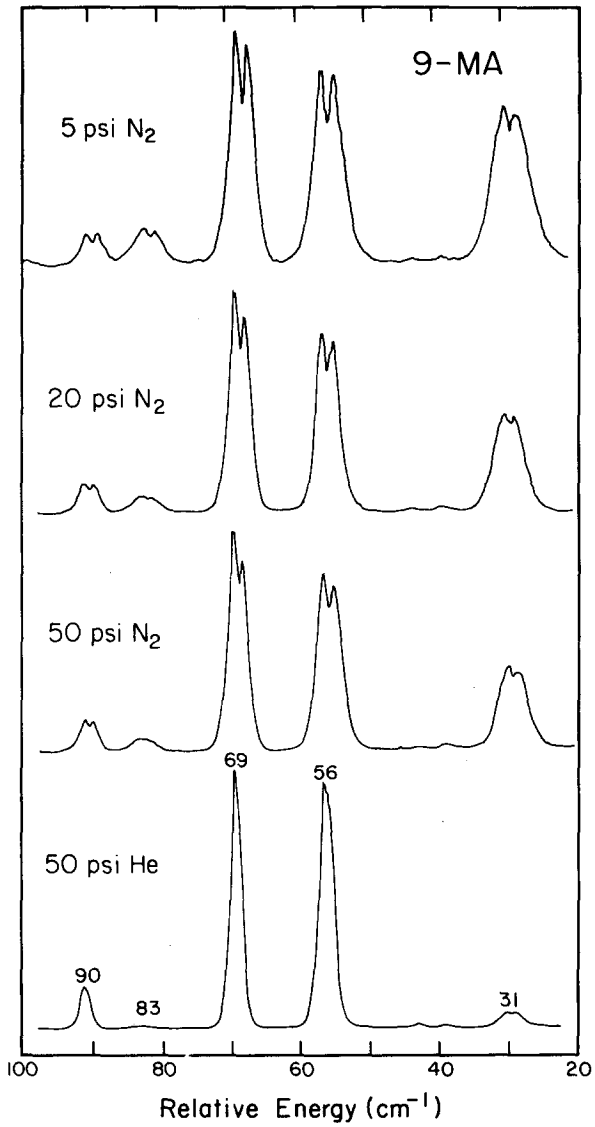

FIG. 8. High resolution spectra of the low frequency region of 9-methylanthracene as a function of carrier gas and backing pressure illustrating the variation of the torsional (hot) band intensity and band shape. Note rotational band splitting. This latter feature was observed and analyzed for anthracene in Ref. 6.

anthryl vs phenyl) this barrier is expected to be even larger. We again employ the simple model for hindered rotation described by Eqs. (1)–(3) using moments of inertia estimated from molecular models for the hexyl and anthryl rotors. For a potential of $V_N \approx 1000$ cm^{-1}, one predicts a vibrational frequency of $\approx$12 cm^{-1}, which is quite consistent with the frequencies observed. Other evidence favoring the assignment of an alkyl–anthryl torsional mode are the observed low frequency intervals of 11 cm^{-1} in A-$(CH_2)_3$-φ[4] and 12 and 16 cm^{-1} in bianthryl.[22]

B. SVL time-resolved spectra: Manifestations of IVR

Direct measurements of the fluorescence decay following SVL excitation in 9-methylanthracene and 9-hexylanthracene were recorded and the rate data plotted in Fig. 10. Also given in Fig. 10 are the fluorescence decay rates measured for anthracene[2] and A-$(CH_2)_3$-φ[4] in earlier studies. The 0^0 level lifetimes measured for 9-MA (21 ns) and 9-HA (18 ns) are similar to those observed for anthracene (21.5 ns)[2] and A-$(CH_2)_3$-φ (20 ns).[4]

In unsubstituted anthracene (and various deuterated derivatives), a general insensitivity of the fluorescence decay rates to vibrational energy was observed above 1800 cm^{-1} [2] (Fig. 10). This behavior was interpreted[2] to be due to a radiationless transition to a nearby electronic state (i.e., a small energy gap process).[23] It was also argued that the constancy of the decay rate above 1800 cm^{-1} was indicative of rapid IVR since this would give rise to decay from a large distribution of states. This conclusion was supported by the onset of completely relaxed fluorescence in the SVL dispersed fluorescence spectra and more importantly by the occurrence of quantum beats *below* this energy region.[3,24]

In the alkylanthracenes, a similar saturation of the decay rate with excess energy was observed, although the onset of this saturation occurs at lower energies (Fig. 10). For the largest molecules, 9-HA and A-$(CH_2)_3$-φ, a plateau is reached at about 400 cm^{-1}. [The decay rates for A-$(CH_2)_3$-φ are only given for energies below 1000 cm^{-1} since a decay channel due to the formation of a charge transfer complex occurs above this energy[4].] In 9-MA,

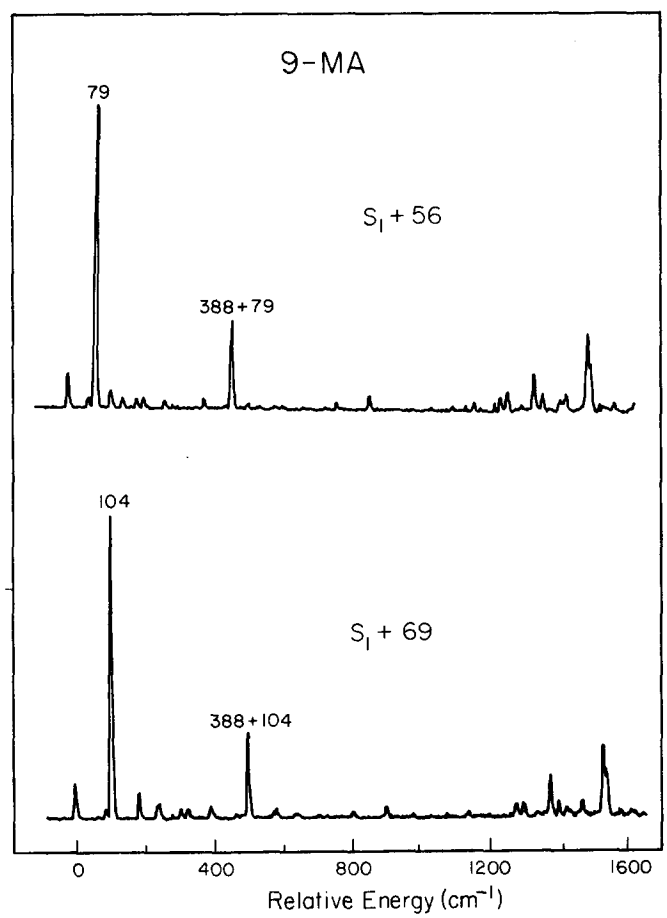

FIG. 9. SVL dispersed fluorescence spectra from S_1 + 56 and S_1 + 69 cm^{-1} showing the association of these modes with the 79 and 104 cm^{-1} vibrations, respectively, in S_0.

Downloaded 21 Sep 2008 to 131.215.225.9. Redistribution subject to AIP license or copyright; see http://jcp.aip.org/jcp/copyright.jsp

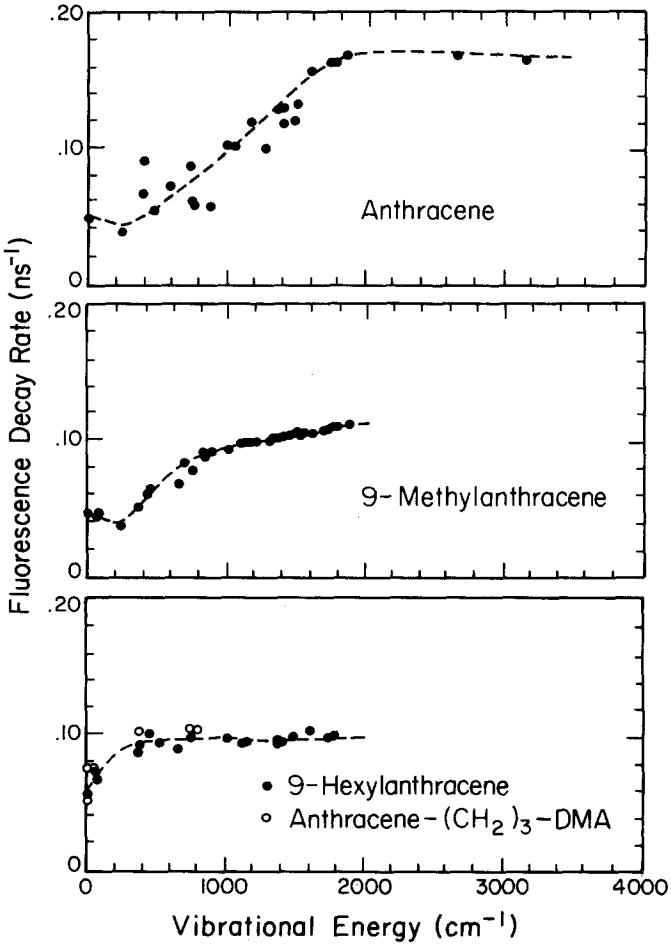

FIG. 10. Observed fluorescence decay rates as a function of vibrational energy in S_1. Comparison of the rates for 9-methyl and 9-hexylanthracene measured in this work are made with our previously measured rates for anthracene (Ref. 2) and A-$(CH_2)_3$-φ (Ref. 4). All rates were measured for expansions involving 35 psi He.

the onset occurs at about 1000 cm^{-1}, however, the higher energy region is not marked by a true saturation, but rather by a slowly increasing decay rate.

C. SVL dispersed fluorescence spectra

The dispersed fluorescence spectra recorded following excitation into single vibronic levels of 9-MA and 9-HA are illustrated in Fig. 11. Certain manifestations of IVR, which are now familiar in SVL dispersed fluorescence spectra of aromatics,[2-5,14,25-27] are evident in Fig. 11. These include; (1) increased broadening and a lack of sharp structure, (2) decreased resonance fluorescence, and (3) red-shifted band shapes.

The SVL fluorescence spectra allow us to make qualitative judgements (with caution) on the *relative* rates of IVR in the substituted anthracenes. On the basis of broadening, one finds that the onset for IVR occurs at lower energies in 9-HA than in 9-MA. This same behavior was observed by Smalley *et al.*[5] in the dispersed fluorescence spectra of jet-cooled alkylbenzenes. This is expected on account of the greater number of vibrations in the longer chain molecules which contribute to a greater density of states. Very low frequency modes are evident (Fig. 1) to support the density of states argument. The onset for IVR in the alkylanthracenes corresponds quite well with the energy at which the decay rates reach a saturation level, in support of the earlier anthracene results and interpretations.[2] However, as emphasized elsewhere,[24,25] the actual rates of IVR cannot be inferred precisely from time integrated fluorescence and can be orders of magnitude slower as recently shown by Felker and Zewail.[24]

IV. DISCUSSION

A. IVR

We examine the threshold and yield of IVR for the anthracene derivatives considered here, by looking to spectral properties which are associated with these effects. The results can then be interpreted in terms of chain dynamics, density of states, and other processes such as the energy dependence of nonradiative decay. Extensive IVR from an initially excited state is commonly reflected by a pronounced broadening in the dispersed fluorescence. These features are evident in Fig. 11, for 9-methylanthracene and 9-hexylanthracene and show that IVR is extensive at energies above 1000 cm^{-1}. Two other observations, however, deserve note; (1) at E_x = 773 cm^{-1}, 9-HA gives a different and broader dispersed fluorescence spectrum than 9-MA and (2) at higher energies, 9-MA gives broader fluorescence bands than 9-HA. These results are treated in the following discussion.

1. Franck-Condon analysis

Although the observation of broadening in fluorescence spectra is viewed as a strong indication of IVR (as

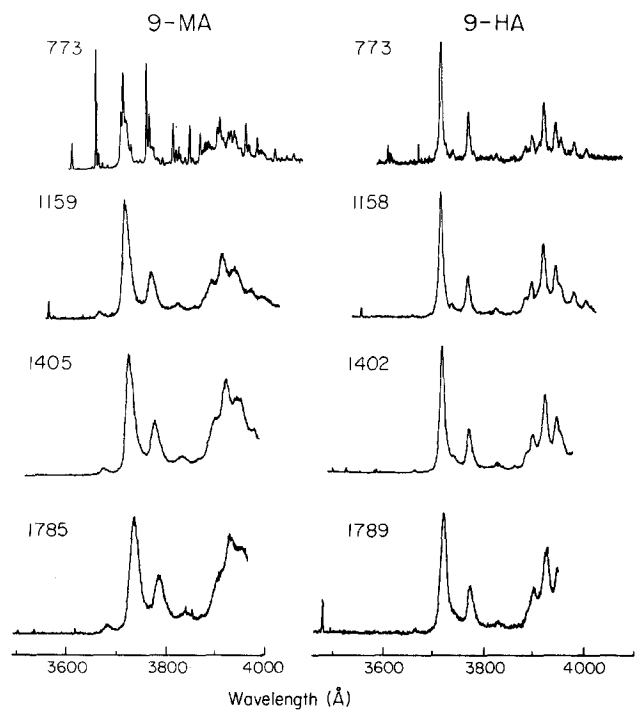

FIG. 11. SVL dispersed fluorescence spectra for 9-methyl and 9-hexylanthracene. Expansion conditions were 35 psi He and monochromator resolution, 1.0 Å. Scattered laser light was used in many spectra (sharp signal at the beginning of each scan) as a wavelength marker.

Downloaded 21 Sep 2008 to 131.215.225.9. Redistribution subject to AIP license or copyright; see http://jcp.aip.org/jcp/copyright.jsp

mentioned earlier), other factors including instrumental resolution and spectral congestion can contribute to a perceived broadening.[24,25] Time-resolved measurements give IVR rates directly.[24] One promising method in time-integrated measurements, which we discuss here, is to use knowledge of the Franck–Condon factors in emission from an optically excited mode to determine the proportion of fluorescence that originates from initial and redistributed states. For instance, a dramatic difference in emission is evident for 9-MA and 9-HA at E_x = 773 cm^{-1} (Fig. 11) even though the same mode is excited (i.e., 12^2). This is presented more systematically in Fig. 12 which contains the dispersed fluorescence spectra of the two molecules following excitation of m = 0, 1, and 2 quanta of the ν_{12} mode.

We have calculated Franck–Condon factors according to the method of Coon *et al.*[28] and Ansbacher[29] as a function of the geometry change along the normal coordinate which we define by a dimensionless parameter γ as

$$\gamma = -\alpha' d \left(\frac{\beta}{1+\beta}\right)^{1/2},$$

$$\beta = \alpha''/\alpha' = \nu''/\nu',$$

$$\alpha^2 = 4\pi^2 \nu/h,$$

where d is the change along a particular vibrational normal coordinate upon an electronic transition, and ν is the vibrational frequency. For values of $\nu' \approx \nu''$, the geometry parameter γ is approximately equal to the amplitude of one quantum of the ground electronic state mode ν''.

Since the vibrational frequencies of the anthracene derivatives are relatively insensitive to the substituent (Table III), we have used the anthracene frequencies, ν'_{12} = 385 cm^{-1} and ν''_{12} = 390 cm^{-1} to calculate the Franck–Condon progression in emission for 9-MA and 9-HA. The results are illustrated in Fig. 12 for a geometry change of γ = 0.55. The calculated 12_n^m progression is clearly evident in the 9-MA spectra up to m = 2 indicating that little emission occurs from bath states. The same behavior was also observed in anthracene.[2,6] The 9-HA spectra, on the other hand, exhibit a 12_n^0 progression built onto a false origin for the 12^1 and 12^2 excitation. The false origin is due to emission from a set of bath modes $\{A\}$. Franck–Condon factors favor emission from states involving no change in the vibrational quantum number (i.e., $m = n$); consequently, the emission following IVR may be described by $\{A_i^i\}\ 12_n^0$. The A_i^i transitions generally exhibit a distribution of frequencies which are similar to the 0_0^0, thus accounting for the broadening and the shift

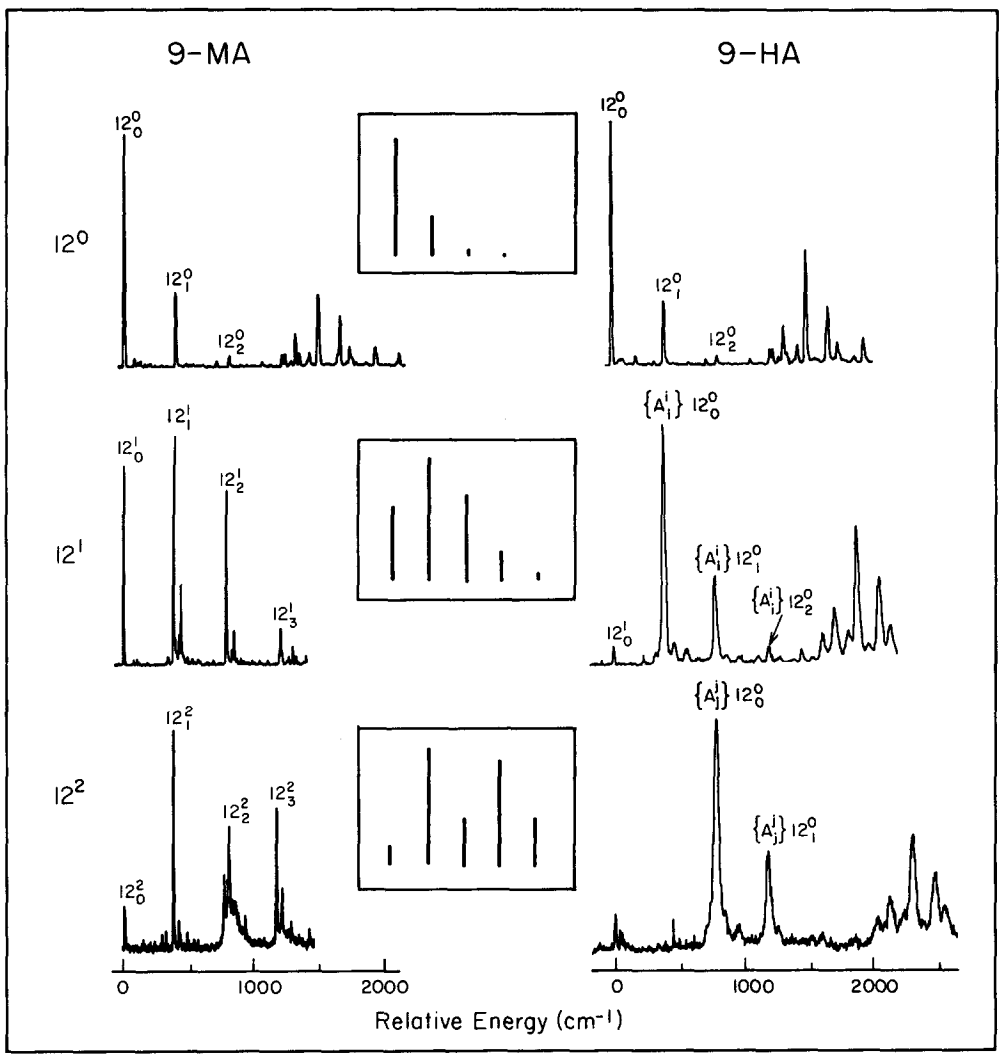

FIG. 12. SVL dispersed fluorscence spectra following excitation into various quanta of the ν_{12} vibration. The calculated Franck–Condon intensity distribution, assuming no IVR, is illustrated in the insert. The calculated spectra agree well with the 9-methylanthracene spectra. The 9-hexylanthracene spectra indicate that the initially excited state redistributes to a set of bath states A before fluorescing. Monochromator resolution was: 9-Methylanthracene; 5 cm^{-1} (12°), 5 cm^{-1} (12^1), 5 cm^{-1} (12^2), 9-Hexylanthracene; 10 cm^{-1} (12°), 15 cm^{-1} (12^1), 15 cm^{-1} (12^2).

Downloaded 21 Sep 2008 to 131.215.225.9. Redistribution subject to AIP license or copyright; see http://jcp.aip.org/jcp/copyright.jsp

of the false origin from the excitation frequency. The predominance of $\{A_i^i\}$ 12_n^0 over 12_n^2 fluorescence in 9-HA indicates that the 12^m level redistributes to the set of bath modes $\{A\}$ on a time that is short compared to the radiative lifetime. This analysis provides additional evidence for IVR, aside from broadening, and leads to the conclusion that IVR is insignificant in 9-MA up to the 12^2 level, yet extensive in 9-HA at only the 12^1 level.

2. *"Long range" redistribution*

Although, IVR in 9-HA is more efficient than in 9-MA, the latter molecule begins to exhibit broader fluorescence bands at higher energies than does 9-HA (Fig. 11). A similar effect was observed in the dispersed fluorescence spectra of alkylbenzenes.[5] The substantial broadening observed for 9-MA could arise from at least two sources: (1) the free rotor properties of the methyl group at high energies which could introduce strong rovibronic coupling; and (2) the differences in frequencies of the (bath) chain vibrations in S_0 and S_1 being greater for 9-MA than for 9-HA. This second point is probable being that most of the hexyl motions are isolated from the anthracene moiety and therefore unaffected by electronic excitation, while the proximity of the methyl group to the anthracene renders it susceptible to the effects of electronic rearrangement.

Other evidence indicating a removal of energy from anthryl groups with long chain substituents is shown in Fig. 13 by the stability of the van der Waals complex of 9-HA with N_2 at energies in excess of 1400 cm^{-1}. This far exceeds the expected anthryl–N_2 bond strength.[30] It is interesting to note in Fig. 13 that under identical cooling conditions, no complex of N_2 with unsubstituted anthracene is evident.

3. *Density of states*

It is possible from the discussion above to identify some energy at which IVR becomes dissipative[24] thus marking the onset of the statistical limit. This so-called threshold energy will depend (among other things) on the density of states that interact with the initially excited state and the strength of this interaction. The combination of these effects is often termed the "effective" density of states.

In anthracene, the IVR threshold was estimated to occur roughly at 1800 cm^{-1}. On the basis of the decay rates, Franck–Condon analysis and broadening in the dispersed fluorescence spectra we can assign this threshold in 9-MA and 9-HA to about 1000 and 400 cm^{-1}, respectively. An IVR threshold of about 400 cm^{-1} or less also appears to hold for A-$(CH_2)_3$-φ.

The correspondence of these threshold energies to some *critical* density of states may be determined by a direct counting procedure[31] and knowledge of the vibrational frequencies of the molecule. In anthracene, we used calculated frequencies[32] since they form a more complete set of modes and do not differ significantly from observed frequencies.[6,11,12] The calculated densities of states are illustrated in Fig. 14 and give a value at the IVR threshold of 1800 cm^{-1} of about 100 per cm^{-1}. We have also presented the calculated density of states for in-plane vibrations for comparison.

The calculation of ρ for the alkylanthracenes is problematic owing to insufficient knowledge of the substituent vibrations. We therefore treat only those low frequency modes that are actually observed in the excitation spectra of 9-MA and 9-HA and consider the calculated density of states to represent lower limits. Therefore, in addition to the anthracene vibrations we include in the calculation for 9-MA the 56 and 69 cm^{-1}

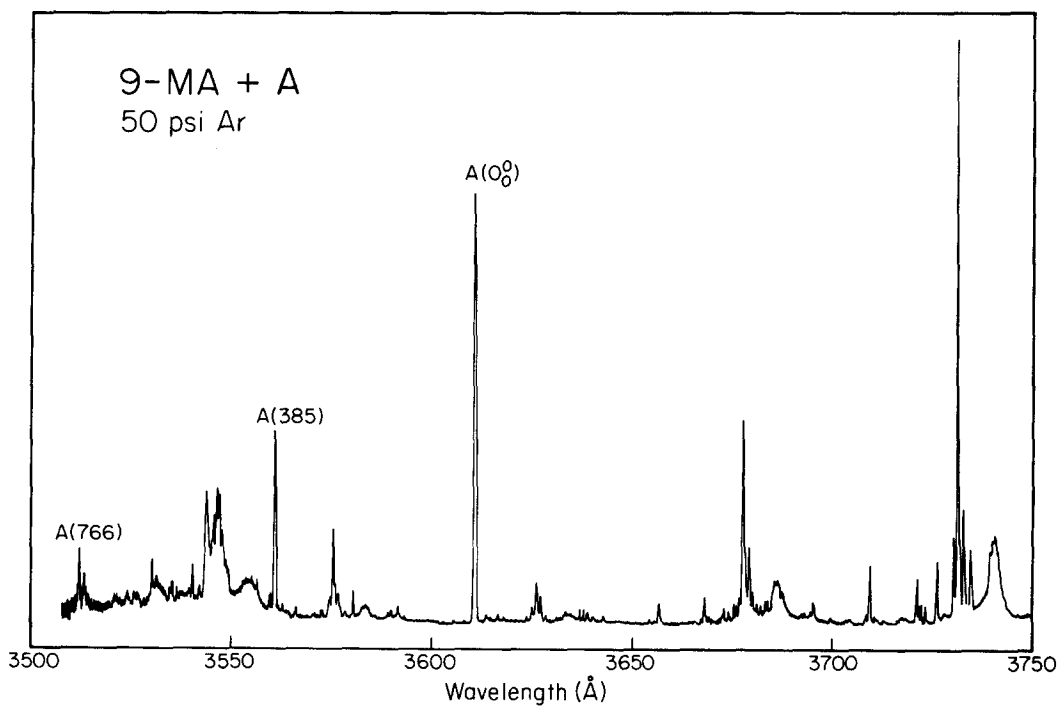

FIG. 13. Excitation spectrum of a mixture of anthracene and 9-hexylanthracene under 50 psi N_2. The spectrum illustrates that van der Waals complexation, which occurs extensively for 9-hexylanthracene, even at high energies, is absent in anthracene under identical expansion conditions.

Downloaded 21 Sep 2008 to 131.215.225.9. Redistribution subject to AIP license or copyright; see http://jcp.aip.org/jcp/copyright.jsp

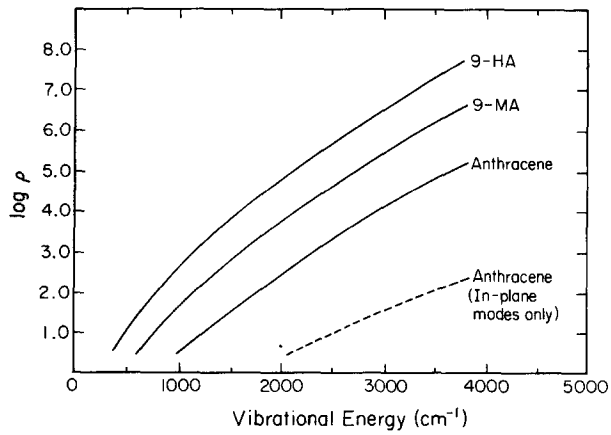

FIG. 14. Density of states calculation. (a) Anthracene; based on calculated values (Ref. 32) for in-plane and out-of-plane vibrations. The calculated result for in-plane vibrations only is also given; (b) 9-methylanthracene; based on the anthracene modes plus the observed modes of 56 and 69 cm^{-1}; (c) 9-hexylanthracene; based on the anthracene modes plus the observed 7 and 36 cm^{-1} modes.

modes and for 9-HA the 7 and 36 cm^{-1} modes. Though underestimating the true density of states, our model is adequate for portraying the general dependence of ρ on E_x which is given in Fig. 14. The calculated lower limits to the critical ρ for 9-MA and 9-HA are about 10 and 40 per cm^{-1}, respectively.

B. Saturation behavior of the decay rates and IVR

The general characteristics of the energy dependent S_1 decay rates for the substituted anthracenes presented in Fig. 10 are (1) energy independent rates above a certain energy (i.e., rate saturation), (2) a "threshold" energy for this saturation effect which varies with the substituent, and (3) mode dependent decay rates below the saturation threshold particularly evident in anthracene.

The threshold for 9-MA is less abrupt than for the other derivatives since the decay rate does not completely saturate, but instead shows a slow rise with energy. We discuss possible reasons for this behavior shortly. The decay behavior for A-$(CH_2)_3$-φ is very similar to 9-HA as expected for a large substituent. [The decay rates for A-$(CH_2)_3$-φ are given below 1000 cm^{-1} only since a decay channel due to the formation of a charge transfer complex occurs above this energy[4].]

It has been demonstrated for some time that electronic states that decay to nearby electronic states can exhibit an energy independent rate of decay[23] provided that *rapid* IVR occurs following vibronic excitation. In cases where IVR is slow, the rate of decay can exhibit mode selectivity depending on the importance of the excited mode in promoting the decay (e.g., through vibronic interactions or Franck–Condon effects). This behavior was observed for anthracene in paper I of this series,[2] which we have presented in Fig. 10. We therefore conclude that the saturation of the decay rates is consistent with IVR that is rapid relative to the lifetime of the state at the excess energies indicated.

The decay rates at saturation illustrated in Fig. 10 decrease for the substituted anthracenes relative to anthracene. This decrease in decay rate may be explanable by an increase in the S–T energy gap. However, calculations on 9-MA indicate that this gap actually decreases (slightly) compared to anthracene.[33] The chain modes may play a role in restricting the rate of ISC by serving as a heat bath which depletes the population of good ISC promoting modes.

Although IVR dynamics in time and frequency resolved spectra are understood in these systems, it appears that the nature of electronic relaxation (i.e., irreversible nonradiative decay due to coupling to other electronic states) is not as fully characterized due to the involvement of triplet states and possible vibronic interactions. Among the interesting manifestations of the electronic relaxation is an inverse isotope effect observed for the anthracene 0^0 level lifetime by this group[2] and Jortner[34] and Lim's groups.[35]

V. CONCLUSION

The dynamics of jet-cooled 9-methyl and 9-hexylanthracene excited to single vibronic levels were investigated. Excitation and 0^0 level dispersed fluorescence spectra were recorded to obtain the vibrations in S_1 and S_0, particularly those attributable to the substituent. SVL decay rates, dispersed fluorescence spectra and Franck–Condon analysis were used to assess the role of alkylation on IVR and to examine properties of the rate saturation behavior observed in all the anthryl molecules. The approximate energies at which the decay rates saturate correspond well with the energy at which fluorescence spectral broadening becomes extensive, these being: anthracene ($\approx$1800 cm^{-1}), 9-MA ($\approx$1000 cm^{-1}), 9-HA ($\approx$400 cm^{-1}), and A-$(CH_2)_3$-φ ($\leq$400 cm^{-1}). IVR dynamics in this series of compounds was discussed in relation to the increased density of states, electronic nonradiative decay, and the saturation behavior of the fluorescence decay rates at increasingly higher excess vibrational energy.

ACKNOWLEDGMENT

We gratefully acknowledge the support of this work by the National Science Foundation.

[1] For a review see (a) A. H. Zewail, Faraday Discuss. Chem. Soc. **75,** 315 (1983); (b) Laser Chem. **2,** 55 (1983); (c) P. M. Felker and A. H. Zewail, in *Applications of Picosecond Spectroscopy to Chemistry,* edited by K. Eisenthal (Reidel, Boston, 1984), p. 273.
[2] W. R. Lambert, P. M. Felker, and A. H. Zewail, J. Chem. Phys. **81,** 2209 (1984).
[3] W. R. Lambert, P. M. Felker, and A. H. Zewail, J. Chem. Phys. **81,** 2217 (1984).
[4] J. A. Syage, P. M. Felker, and A. H. Zewail, J. Chem. Phys. **81,** 2233 (1984).
[5] (a) J. B. Hopkins, D. E. Powers, and R. E. Smalley, J. Chem. Phys. **72,** 5039 (1980); (b) **73,** 683 (1980).
[6] W. R. Lambert, P. M. Felker, J. A. Syage, and A. H. Zewail, J. Chem. Phys. **81,** 2195 (1984).
[7] (a) H. P. Rudolph, H. Dreizler, A. Jaeschke, and P. Wendling, Z. Naturforsch. Teil A **22,** 940 (1967); (b) W. A. Kreiner, H. D. Rudolph, and B. T. Tan, J. Mol. Spectrosc. **48,** 86 (1973).
[8] J. Murakami, M. Ito, and K. Kaya, Chem. Phys. Lett. **80,** 203 (1981).
[9] B. W. Keelan, J. A. Syage, J. F. Shepanski, and A. H. Zewail, *International Conference on Lasers '83, Society for Optical and Quantum Electronics, Virginia* (STS, McLean, VA, 1985), p. 718.
[10] R. Pariser, J. Chem. Phys. **24,** 250 (1956).
[11] A. Bree and S. Katagiri, J. Mol. Spectrosc. **17,** 24 (1965).

Downloaded 21 Sep 2008 to 131.215.225.9. Redistribution subject to AIP license or copyright; see http://jcp.aip.org/jcp/copyright.jsp

[12] G. J. Small, J. Chem. Phys. **52,** 656 (1970).
[13] M. Stockburger, H. Gattermann, and W. Klusmann, J. Chem. Phys. **63,** 4519 (1975).
[14] (a) S. M. Beck, D. E. Powers, J. B. Hopkins, and R. E. Smalley, J. Chem. Phys. **73,** 2019 (1980); (b) S. M. Beck, J. B. Hopkins, D. E. Powers, and R. E. Smalley, J. Chem. Phys. **74,** 43 (1981).
[15] U. Even and J. Jortner, J. Chem. Phys. **78,** 3445 (1983), and references therein; see also A. Amirav, U. Even, and J. Jortner, J. Chem. Phys. **75,** 3770 (1981).
[16] (a) T. R. Hays, W. Henke, H. L. Selzle, and E. W. Schlag, Chem. Phys. Lett. **77,** 19 (1981); (b) K. Godzik, T. R. Hays, W. E. Henke, H. L. Selzle, E. W. Schlag, and S. H. Lin, Laser Chem. **1,** 59 (1982); (c) W. Yu, W. E. Henke, H. L. Selzle, E. W. Schlag, D. Wutz, and S. H. Lin (to be published).
[17] H. C. Longuet-Higgins, Mol. Phys. **6,** 445 (1963).
[18] A. V. Cunliffe, *Internal Rotations in Molecules,* edited by W. J. Orville Thomas (Wiley, New York, 1974), Chap. 7.
[19] D. G. Lister, J. N. MacDonald, and N. C. Owen, *Internal Rotation and Inversion* (Academic, New York, 1978).
[20] J. A. Syage, P. M. Felker, and A. H. Zewail, J. Chem. Phys. **81,** 4685 (1984).
[21] (a) R. K. Harris and M. Thorley, J. Mol. Spectrosc. **42,** 407 (1972); (b) M. Camail, A. Protiere, and H. Bodet, J. Phys. Chem. **79,** 1966 (1975); (c) P. Scharfenberg, B. Rozsondai, and I. Hargittai, Z. Naturforsch. Teil A **35,** 431 (1980).
[22] Unpublished work from this laboratory.
[23] See, e.g., S. Fischer, E. W. Schlag, and S. Schneider, Chem. Phys. Lett. **11,** 583 (1971).
[24] (a) P. M. Felker and A. H. Zewail, Chem. Phys. Lett. **102,** 113 (1983); (b) **108,** 303 (1984); (c) Phys. Rev. Lett. **53,** 501 (1984).
[25] J. A. Syage, P. M. Felker, and A. H. Zewail, J. Chem. Phys. **81,** 4706 (1984).
[26] P. S. H. Fitch, L. Wharton, and D. H. Levy, J. Chem. Phys. **70,** 2018 (1979).
[27] A. Amirav, U. Even, and J. Jortner, J. Chem. Phys. **74,** 3745 (1981).
[28] J. B. Coon, R. E. DeWames, and C. M. Loyd, J. Mol. Spectrosc. **8,** 285 (1962).
[29] F. Ansbacher, Z. Naturforsch. Teil A **14,** 889 (1959).
[30] Since van der Waals complexes involving anthracene are more efficiently formed with Ar than with N_2, the binding energy for the latter is expected to be less than the value of ≈ 500 cm^{-1} estimated for anthracene–Ar [Ref. 16(c)].
[31] W. L. Hase and D. L. Bunker, program QCPE-234, Caltech, Pasadena, CA.
[32] (a) K. Ohno, J. Mol. Spectrosc. **77,** 329 (1979); (b) D. J. Evans and D. B. Scully, Spectrochim. Acta **20,** 891 (1964).
[33] Ch. Jung and K.-H. Heckner, Chem. Phys. **21,** 227 (1977).
[34] (a) A. Amirav, M. Sonnenschein, and J. Jortner, Chem. Phys. Lett. **100,** 488 (1983); (b) **102,** 573 (1983).
[35] S. Okajima, B. E. Forch, and E. C. Lim, J. Phys. Chem. **87,** 4571 (1983).

Downloaded 21 Sep 2008 to 131.215.225.9. Redistribution subject to AIP license or copyright; see http://jcp.aip.org/jcp/copyright.jsp